

CHARACTERISTICS OF GZO/IZO DUAL-LAYER AS AN ELECTRON TRANSPORT LAYER IN DYE-SENSITIZED SOLAR CELL

GZO/IZO semiconductor thin films were prepared on the ITO substrate via sol-gel spin coating method for using in the dye-sensitized solar cells (DSSCs). For this purpose, GZO and IZO thin films were optimized by the percentage of doping gallium and indium in zinc oxide and were studied their electrical, optical and structural properties. After that, the layers with the best performance were selected for use in the DSSCs. The concentration of all solutions for spin coating processes was 0.1 M and zinc oxide has been doped with gallium and indium, with different doping percentages (0, 0.5, 1, 2 and 4 volume percentage). So, by studying the properties of the fabricated thin films, it was found the films with 0.5%GZO and 0.5%IZO have the best performance and hence, the optimized dual-layer (0.5% GZO/0.5% IZO (GIZO)) were prepared and studied their electrical and optical properties. The synthesized optimized dual-layer film was successfully used as the working electrode for dye-sensitized solar cells. The sample with 0.5%IZO shows the 9.1 mA/cm² short-circuit current density, 0.52 V open circuit voltage, 63% fill factor and 2.98% efficiency.

Keywords: Dual-layer, Sol-gel, Spin coating, Thin film, GIZO, Solar Cell

1. Introduction

The world's leading technologies are photovoltaic systems and thin layers. Wide developments in thin film technology such as thin film [1,2] and dye-sensitized solar cells are introduced. In these solar cells, a transparent conductive oxide is used as an electron-conducting material. Transparent metal oxide thin films are extensively served for a wide range of optoelectronic devices such as working electrodes in the flat screens, flexible touch displays, anti-static electricity layers, and thin film solar cells because of their high electrical conductivity and transparency. Among the variety of thin films, semiconductor-based transparent conductive ZnO had a much attention, because of its amazing features such as relatively inexpensive and accessible, sustainable, environmentally, high transparency, lightweight and also owing excellent optical, electrical, chemical properties, high carrier mobility, better chemical stability and low light sensitivity level [3-6]. Thus, these films can be used as active layers in transparent electrode applications, solar cells, and optoelectronic devices to improve electrical and optical performance. The properties of these semiconductors can be changed by adding impurities [7]. Physical properties of ZnO thin films are depended on doping and hence a systematic study of the effects of doping on the physical, electrical and optical properties is very important for many scientific applications. The elements of Group III (B, Al, Ga, In and ...) can be added to n-type ZnO as impurity [8]. These elements that can improve

the electrical and optical properties of ZnO thin films act as an effective donor. ZnO thin films doped with aluminum, gallium, and indium have a higher electrical conductivity, higher stability and resistivity rather than pure zinc oxide films [9]. Due to indium is a charming impurity for n-type ZnO and has less reactive and greatest resistivity than other its group elements, was selected for doping in the ZnO structure. Also, indium doped ZnO has many advantages like that high light transmission, high electrical conductivity, and high thermal stability. Also, gallium has ionic radius nearest the Zn one that doesn't change the crystal phase of ZnO. There are many physical and chemical methods for synthesis of impurity doped zinc oxide, such as; chemical vapor deposition (CVD) [10], molecular beam epitaxy [11], electron beam evaporation [12], pulsed laser deposition [13], sputtering [14], RF sputtering [15], reactive evaporation [16] and sol-gel [17]. Among these methods, sol-gel is a wet chemical process based on the desirable solution and is used because of the simplicity, low cost, large area coverage, easy control of doping level, synthesis of high purity and does not require vacuum equipment. Quite clear sol concentration and annealing temperature have a significant effect on the physical and electrical properties of thin films prepared by this method. In this study, the effect of doping value of gallium and indium into ZnO structure on the structure, electrical and optical properties of prepared films were examined. Also, the optimum dual layer of GZO/IZO, with the highest yield as an electron transport layer was fabricated for use in dye-sensitized solar cells.

* VALI-E-ASR UNIVERSITY OF RAFSANJAN, FACULTY OF SCIENCE, DEPARTMENT OF PHYSICS, RAFSANJAN 7718897111, IRAN

** VALI-E-ASR UNIVERSITY OF RAFSANJAN, FACULTY OF SCIENCE, DEPARTMENT OF CHEMISTRY, RAFSANJAN 7718897111, IRAN

Corresponding author: mehdi_ahmadi79@yahoo.com

2. Experimental

2.1. Synthesized of GZO and IZO thin films

All chemicals were high purity and supplied by Merck and Aldrich Company. Zinc acetate dihydrate ($\text{Zn}(\text{CH}_3\text{COO})_2 \cdot 2\text{H}_2\text{O}$), ethanol ($\text{C}_2\text{H}_6\text{O}$), 2-methoxy ethanol ($\text{C}_3\text{H}_8\text{O}_2$), 2-propanol ($\text{C}_3\text{H}_8\text{O}$), monoethanolamine ($\text{C}_2\text{H}_7\text{NO}$), gallium nitrate ($\text{Ga}(\text{NO}_3)_3$), and indium nitrate ($\text{In}(\text{NO}_3)_3 \cdot x\text{H}_2\text{O}$) were used as received without further purifications. In an experimental procedure 0.216g zinc acetate dehydrate was dissolved in 10 ml 2-propanol and 1ml monoethanolamine was added to the solution as a stabilizer. The obtained solution was stirred at 70°C for one hour until a clear and stable sol was created. After that for preparation of gallium and indium solutions, 0.212 g of gallium nitrate and 0.105 g of indium nitrate were dissolved in 10 ml of ethanol, separately and then 1 ml of 2-methoxy ethanol was added to each solution as a stabilizer. After that, the gallium and indium solutions were added to the ZnO one with 0.5, 1, 2 and 4 volume percentage and were stirred for 20 minutes to obtain transparent solutions of gallium-doped ZnO (GZO) and indium-doped ZnO (IZO). To fabricate of thin films with each obtained solution, ITO glass substrates were washed with distilled water, acetone and isopropanol alcohol by ultrasonic for 10 minutes respectively, and were dried by argon gas. Then, the layers were deposited by the spin coating technique with speed of 2500 rpm for 25 s and were annealed in the 200°C temperature for 1h.

2.2. Synthesized of GZO/IZO (GIZO) dual-layer

By knowing the optimal layer, to obtain GIZO dual-layer, first 0.5% GZO solution was deposited on the ITO glass substrate (2×2cm) for 25 s and were annealed at 200°C for 1 hour and then slowly cooled. After that, 0.5% IZO solution was deposited on GZO layer for 25 s, and the samples were annealed at 500°C for 30 min for using in DSSC.

The electrical, optical and structural of thin films were studied by XRD, SEM, UV-Vis spectrometer and four-point probe technique. XRD patterns were recorded by a Rigaku D-max C III, X-ray diffractometer using Ni-filtered Cu K_α radiation. Scanning electron microscopy (SEM) images were obtained on Philips XL-30ESEM equipped with an energy dispersive X-ray spectroscopy. UV-Vis spectra were recorded using a UV-Vis spectrophotometer (PerkinElmer). The electrical conductivities were measured by a two-point layout with a KEITHLEY 236 Source Measure Unit.

3.2. Fabrication of dye-sensitized solar cell

To fabricate the dye-sensitized solar cell, the obtained GIZO layer was deposited on the ITO glass substrate as an electron transition layer and then was inserted into the N719 dye solution for 72 h. The prepared platinum thin film deposited on the

ITO was selected as a counter electrode and before using it was annealed at 500°C for 30 min. After that both prepared layer (working and counter electrodes) were connected together by a thin layer of surlyn and by very small holes on the counter electrode, the electrolyte was injected to the solar device and the holes were covered with surlyn layer to prevent electrolyte leakage. The prepared cell was characterized by I-V curve via a solar simulator and I-V meter. For illumination, an Oriol Sol 1A solar simulator was used to provide an AM1.5G spectrum at 100 mW/cm².

3. Results

3.1. Optical properties of thin films

Fig. 1(a), (b) and (c) showed the transmittance of GZO, IZO and GIZO samples, respectively. It was found that all prepared samples are transparent in the visible range (400- 800 nm) and by increasing the doping value the transparency is improved. Also, it was found that the sample with 0.5% GZO and 0.5% IZO has the highest transmittance percentage and subsequently has the best optical performance. So it can be said that the prepared dual layer thin film can be used in the optical devices. The average and maximum of transmittance percentage of the samples were shown in Table 1.

TABLE 1

The average and the maximum transmittance of 0-4% GZO, IZO and GIZO thin films at 300-800 nm

Sample	Average transmittance (%)	Max transmittance (%)
ZnO	86.46	91.87
0.5%GZO	93.15	98.63
1%GZO	92.86	98.51
2%GZO	92.27	98.00
4%GZO	92.51	98.22
0.5%IZO	93.50	98.9
1%IZO	93.00	98.5
2%IZO	92.59	98.3
4%IZO	92.51	98.3
0.5GIZO	86.83	95.5
1%GIZO	85.70	95
2%GIZO	85.84	95.4
4%GIZO	86.37	95.2

3.2. SEM images

Fig. 2 shows the SEM images of the thin films prepared from pure ZnO (2a), 0.5% GZO (2b), 0.5% IZO (2c) and GIZO (d). As it can be seen all samples are composed of spherical particles and the uniformity of the particles was improved by doping gallium and indium. Also, it can be observed the average size of particles was increased in 0.5% IZO sample and decreased in the 0.5% GZO and optimized GIZO samples. In fact, it can

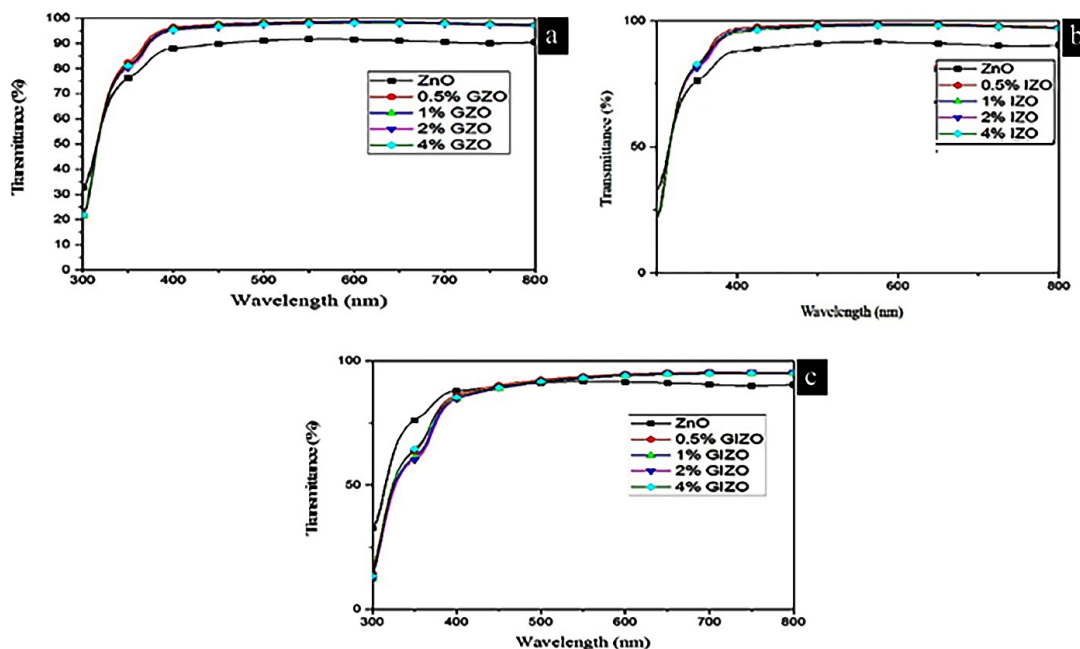


Fig. 1. The transmittance property of 0-4% GZO (a), IZO (b) and GIZO (c) thin films

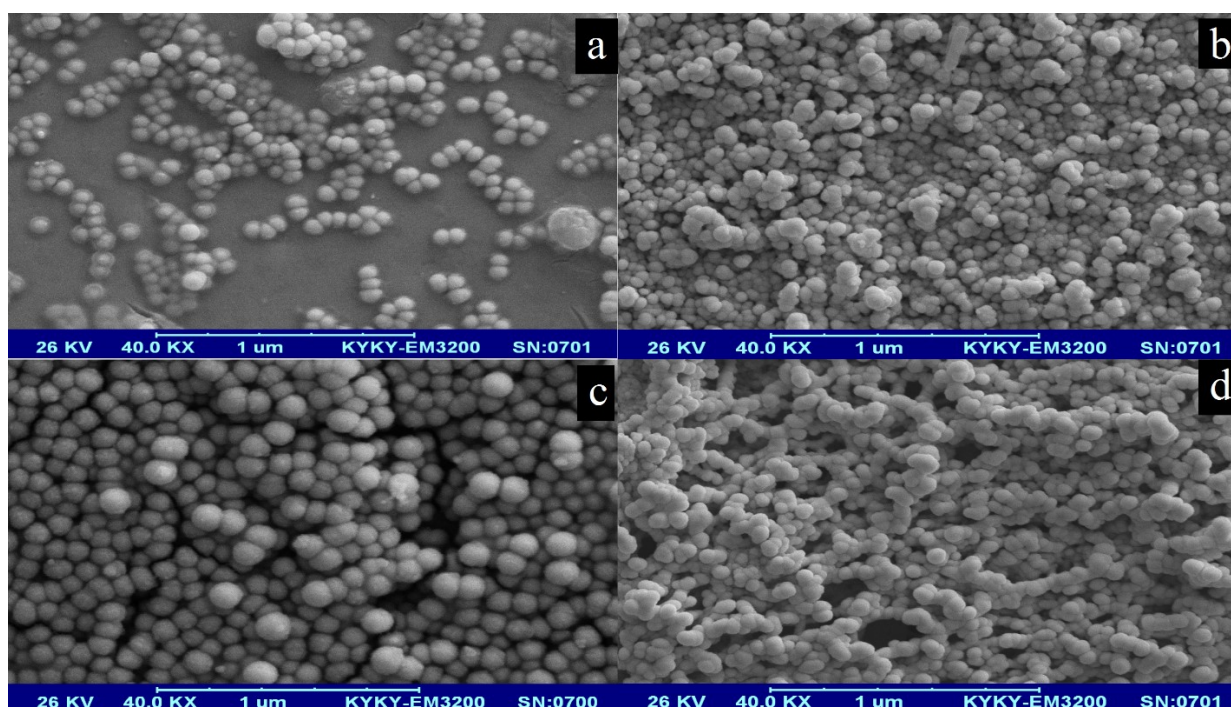


Fig. 2. SEM images of pure ZnO (a), 0.5%GZO (b), 0.5%IZO (c) and GIZO (d) thin films

be said that by adding the impurity the nucleation rate of ZnO nucleus was changed and hence different particles sized were obtained. The estimated particles size of the prepared thin films were 20-50 nm.

3.3. Calculation of the energy band gap

The band gap of thin layers from UV-Vis data was calculated by the following equation [18]:

Equation (1):

$$\alpha h\nu = A(h\nu - E_g)^n$$

Where E_g is the band gap, A is the constant, α is the absorption coefficient, $h\nu$ is incident photon energy and $n = 2$ is for the indirect gap and $n = 0.5$ for the direct gap. The band gap of the thin films can be calculated by extrapolation of the obtained curve to the energy axis (Fig. 3).

Table 2 shows the energy band gap of the samples IZO (3a), GZO (3b) and GIZO (3c), respectively. It was found that

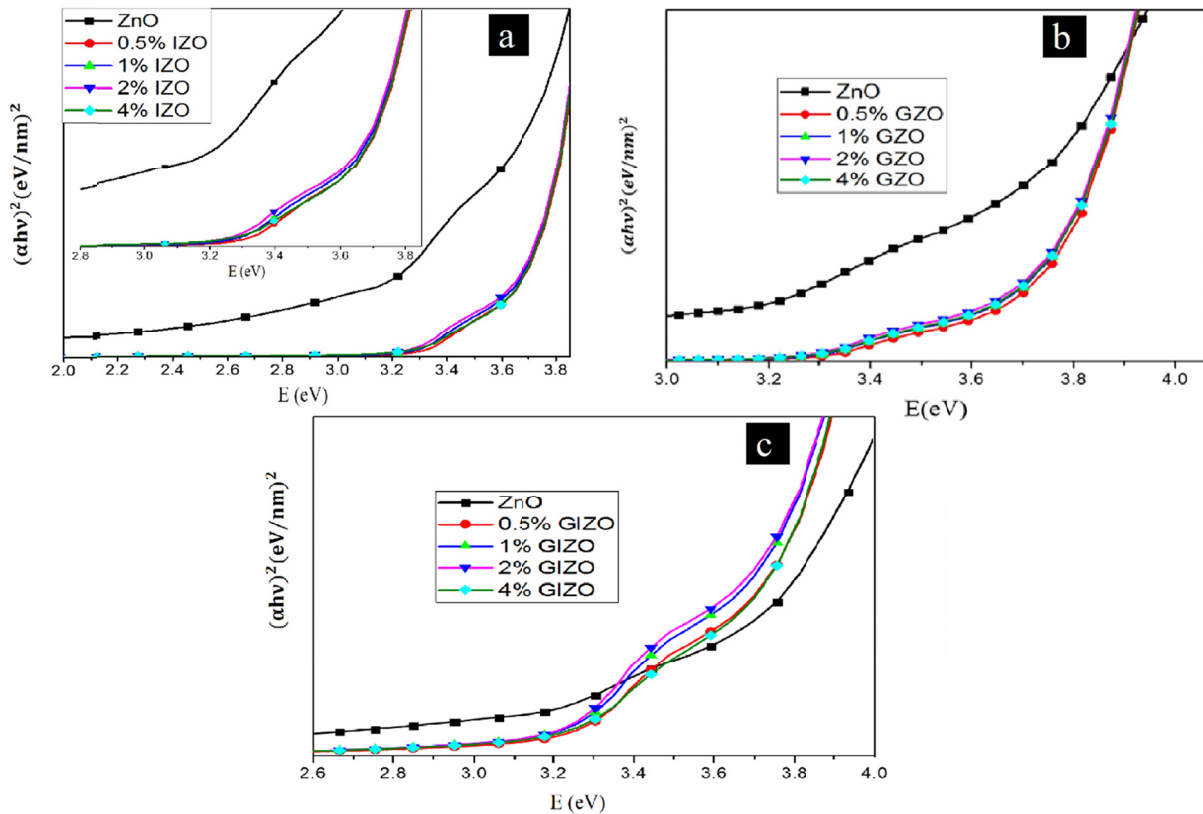


Fig. 3. The optical band gap of 0-4% IZO (a), GZO (b) and GIZO (c) thin films

the samples with 0.5% GZO and 0.5% IZO have the highest band gap value. Also, the redshift of band gaps can be related to the increase of carrier concentration with impurity doping [19].

TABLE 2

The optical band gap of 0-4% GZO, IZO and GIZO thin films

Sample	Band gap
ZnO	3.47
0.5%GZO	3.71
1%GZO	3.68
2%GZO	3.63
4%GZO	3.67
0.5%IZO	3.62
1%IZO	3.59
2%IZO	3.58
4%IZO	3.6
0.5GIZO	3.4
1%GIZO	3.37
2%GIZO	3.35
4%GIZO	3.41

3.4. X-ray diffraction pattern

Fig. 4 shows the X-ray diffraction patterns of pure ZnO (4a), Ga-doped ZnO (4b), In-doped ZnO (4c) and GIZO (4d) nanocrystalline thin films. It can be seen that there are strong diffraction peaks at 31.65° , 34.35° and 36.15° which correspond to the [100], [002] and [101] Miller indices respectively. Also, it

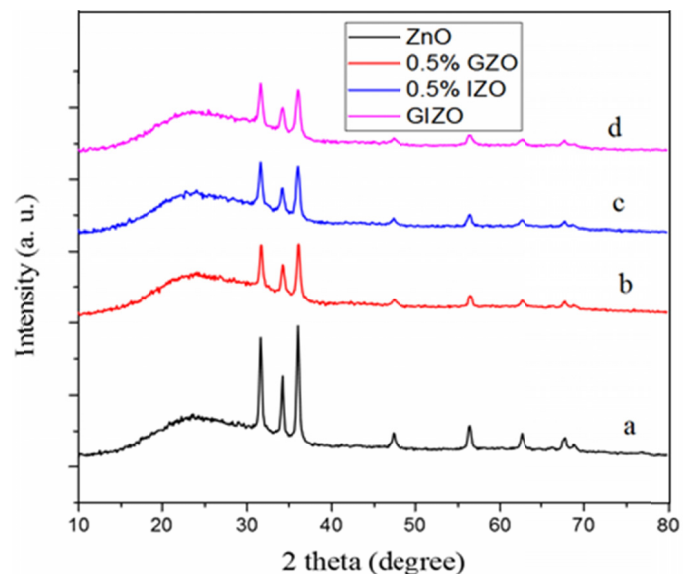


Fig. 4. X-ray diffraction patterns of pure ZnO (a), 0.5%GZO (b), 0.5%IZO (c) and GIZO (d) thin films

was found the crystal structure of ZnO is not changed by doping gallium and indium. In other words, all samples have wurtzite hexagonal structures like the ZnO one. As it can be seen the XRD patterns of GZO, IZO and GIZO samples have a small displacement to the lower angle respect to the ZnO pure one that approves the occupation of Zn^{2+} location by the gallium and indium ions. Doping of Ga and In atoms in ZnO does not cause structural metamorphosis, but, since In^{3+} and Ga^{3+} have an

ionic radius larger compared to Zn^{2+} , by replacing Ga and In ions instead of Zn one, the lattice constants are reduced [20]. It can be observed that by increasing the doping value, the diffraction peak intensity of GZO and IZO films respect to the pure ZnO is decreased. The full width at half maximum (FWHM) of all peaks in GZO, IZO and GIZO patterns, is wider than the pure ZnO pattern. Since the narrow FWHM and stronger diffraction intensity means better crystal quality, so this shows that by doping In and Ga ions in ZnO lattice the crystallinity of ZnO is decreased. This can be attributed to the differences in the size of Zn ions and the impurity ions [7].

3.5. Electrical resistance and conductivity

Due to replacing some Zn ions with In and Ga ones, the free electron density is increased and therefore, the doped films have lower resistance compared to the un-doped films. The electrical resistance of all samples has been measured by four-point probe technique. Table 3 shows the electrical conductivity of 0-4% GZO, IZO and also GIZO samples. The higher conductivity of the films after doping the optimum value of Ga and In can be explained by the fact that the Ga and In ions localized in the ZnO lattice act as donor centers and induce native n-type conductivity in ZnO film and also reduce the oxygen vacancy.

TABLE 3

The electrical conductivity of 0-4% GZO, IZO and also GIZO samples

Sample	Electrical conductivity (S/cm)
ZnO	9×10^{-5}
0.5%GZO	3×10^{-4}
0.5%IZO	2×10^{-4}
0.5GIZO	4×10^{-9}
1%GIZO	1×10^{-8}
2%GIZO	2×10^{-8}
4%GIZO	8×10^{-9}

3.6. J-V curve analysis DSSCs

One of the important characterization to investigate the solar cells behavior is the current-voltage curve. The important electrical characteristics of a solar cell include the following; V_{oc} : open circuit voltage, J_{sc} : short circuit current, FF : fill factor ($FF = (J_{max} \cdot V_{max}) / (J_{sc} \cdot V_{oc})$) and σ : power conversion efficiency ($\sigma = P_{out} / P_{in} = (J_{sc} \cdot V_{oc}) / P_{high}$) (P_{in} = input power; P_{out} = output power; P_{high} = the highest power). Fig. 5 shows the J-V curve of the samples and also, Table 4 shows the calculated of σ , J_{sc} , V_{oc} and FF of the samples. It can be seen that power conversion efficiency (σ) for the cell with 0.5% IZO is higher than for the other samples. The better solar cell parameters can be related to the mono-layer and different morphologies of this sample respect to the other samples.

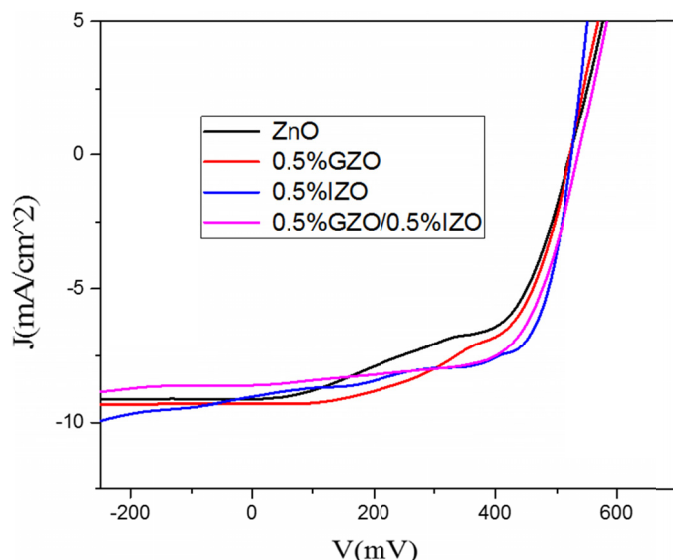


Fig. 5. Current-Voltage characteristics graph of the solar cells (cell area = 0.25 cm²) for ZnO, 0.5%GZO, 0.5%IZO and 0.5%GIZO

TABLE 4

Cell parameters of the dye sensitized solar cells

Sample	V_{oc} (mV)	J_{sc} (mA/cm ²)	FF	σ (%)
ZnO	0.52	9.1	0.53	2.50
0.5%GZO	0.53	9.3	0.55	2.67
0.5%IZO	0.52	9.1	0.63	2.98
0.5GIZO	0.53	8.6	0.62	2.82

4. Conclusion

In this research, pure ZnO thin films and also Ga-doped ZnO and In-doped ZnO with different doping percentages (0.5, 1, 2 and 4%) were prepared by using sol-gel method and spin coating technique. The results showed all layers have optical transmittance top of 90% in the visible region and the highest optical transmittance is belong to the thin film with 0.5% GZO and 0.5% IZO samples. So, they can be appropriate for use in the optical applications. The results of SEM images showed that the prepared surfaces have good uniformity and by doping due to change of nucleation rate, the prepared surfaces have different particles sizes. The UV-Vis results showed that the films with 0.5% GZO and 0.5% IZO have the highest energy band gap. From the XRD patterns, it was found that Ga and In ions were successfully doped in the ZnO nanostructure with wurtzite phase. It was found that the films with 0.5% GZO and 0.5% IZO were appropriate for use in dye-sensitized solar cell and it was found the prepared cell had good performance with 2.98% efficiency.

REFERENCES

- [1] M. Sabet, M. Salavati-Niasari, M. Ashjari, D. Ghanbari, M. Dadkhah, Journal of Inorganic and Organometallic Polymers and Materials **22**, 1139-1145 (2012).

- [2] M. Sabet, M. Salavati-Niasari, D. Ghanbari, O. Amiri, N. Mir, M. Dadkhah, *Materials Science in Semiconductor Processing* **25**, 98-105 (2014).
- [3] S.M. Lee, Y.H. Joo, Ch. Kim, *Appl. Surf. Sci.* **320**, 494-501 (2014).
- [4] L. Cui, G.G. Wanga, H.Y. Zhanga, R. Suna, X.P. Kuanga, J. Cai, *Ceram. Int.* **39**, 3261-3268 (2013).
- [5] M. Ajili, M. Castagn, N.K. Turki, *Superlattice. Microst.* **53**, 213-222 (2013).
- [6] Ch.Y. Tsayn, W.T. Hsu, *Ceram. Int.* **39**, 7425-7432 (2013).
- [7] Ch.Y. Tsaya, K.Sh. Fana, Ch.M. Lei, *J. Alloy. Comp.* **512**, 216-222 (2012).
- [8] J. Li, J. Xu, Q. Xu, G. Fang, *J. Alloy. Comp.* **542**, 151-156 (2012).
- [9] M. Thambidurai, J.Y. Kim, Ch. Kang, N. Muthukumarasam, H.J. Song, J. Song, Y. Ko, D. Velauthapillai, Ch. Le, *Renew. Energ.* **66**, 433-442 (2014).
- [10] B. Loukya, D.S. Negi, R. Sahu, N. Pachauri, A. Gupta, R. Datta, *J. Alloy. Comp.* **668**, 187-193 (2016).
- [11] T.Y. Wu, Y.S. Huang, S.Y. Hu, Y.C. Lee, K.K. Tiong, C.C. Chang, J.L. Shen, W.C. Chou, *Solid. State. Comm.* **237-238**, 1-4 (2016).
- [12] H.K. Park, J. Jo, H.K. Hong, G.Y. Song, J. Heo, *Curr. Appl. Phys.* **15**, 964-969 (2015).
- [13] F. Mitsugi, Y. Umeda, N. Sakai, T. Ikegami, *Thin Solid Films* **518**, 6334-6338 (2010).
- [14] Z. Zhang, Y. Tang, J. Chen, J. Chen, *Phys. B. Condens. Matter.* **495**, 76-81 (2016).
- [15] A.I. Savchuk, V.V. Strebezhev, G.I. Kleto, Y.B. Khalavka, I.M. Yuriyichuka, P.M. Fochuk, V.M. Strebezhev, *Surf. Coating. Tech.* **295**, 8-12 (2016).
- [16] G. Sahoo, S.R. Meherb, M.K. Jain, *Mater. Sci. Eng. B.* **191**, 7-14 (2015).
- [17] L. Qian, L. Xifeng, Zh. Jianhua, *J. Alloy. Comp.* **572**, 175-179 (2013).
- [18] S. Salari, M. Ahmadi, K. Mirabbaszadeh, *Elec. Matt. Lett.* **10**, 13-20 (2014).
- [19] M. Dutta, S. Mridha, D. Basak *Appl. Surf. Sci.* **254**, (2008) 2743-2747.
- [20] Z.N. Ng, K.Y. Chan, Ch.Y. Low, Sh. A. Kamaruddin, M.Z. Sahdan, *Ceram. Int.* **41**, S254-S258 (2015).